J Solid State Electrochem (2012) 16:2651–2660
DOI 10.1007/s10008-012-1684-9

ORIGINAL PAPER

NO_x conversion on porous LSF15–CGO10 cell stacks with KNO_3 or K_2O impregnation

M. L. Traulsen · F. Bræstrup · K. Kammer Hansen

Received: 1 December 2011 / Revised: 6 February 2012 / Accepted: 8 February 2012 / Published online: 28 February 2012

Abstract In the present work, it was investigated how addition of KNO_3 or K_2O affected the NO_x conversion on LSF15–CGO10 ($La_{0.85}Sr_{15}FeO_3$–$Ce_{0.9}Gd_{0.1}O_{1.95}$) composite electrodes during polarization. The LSF15–CGO10 electrodes were part of a porous 11-layer cell stack with alternating layers of LSF15–CGO10 electrodes and CGO10 electrolyte. The KNO_3 was added to the electrodes by impregnation and kept either as KNO_3 in the electrode or thermally decomposed into K_2O before testing. The cell stacks were tested in the temperature range 300–500 °C in 1,000 ppm NO, 10% O_2, and 1,000 ppm NO+10% O_2. During testing, the cells were characterized by electrochemical impedance spectroscopy, and the NO conversion was measured during polarization at −3 V for 2 h. The concentration of NO and NO_2 was monitored by a chemiluminescence detector, while the concentration of O_2, N_2, and N_2O was detected on a mass spectrometer. A significant effect of impregnation with KNO_3 or K_2O on the NO_x conversion was observed. In 1,000 ppm NO, both impregnations caused an increased conversion of NO into N_2 in the temperature range of 300–400 °C with a current efficiency up to 73%. In 1,000 ppm NO+10% O_2, no formation of N_2 was observed during polarization, but the impregnations altered the conversion between NO and NO_2 on the electrodes. Both impregnations caused increased degradation of the cell stack, but the exact cause of the degradation has not been identified yet.

Keywords Exhaust gas cleaning · NO_x removal · NO_x reduction · $deNO_x$ · Impregnation · LSF

M. L. Traulsen (✉) · F. Bræstrup · K. K. Hansen
Fuel Cells and Solid State Chemistry Division,
Risø National Laboratory for Sustainable Energy,
Technical University of Denmark,
4000 Roskilde, Denmark
e-mail: matr@risoe.dtu.dk

Introduction

NO_x is an air pollutant, which has a number of negative effects on human health and the environment, as NO_x affects the respiratory system negatively, increase the formation of ozone at ground level, cause formation of acid rain, contribute to smog formation, and also act as green house gas [1]. In gasoline vehicles, NO_x can be removed sufficiently from the exhaust by the three-way-catalyst, but this catalyst does not work for diesel vehicles due to higher oxygen content in diesel engine exhaust [2]. For this reason, other technologies are used for NO_x removal from diesel engine exhaust, the three most well-known technologies being selective catalytic reduction with urea (urea-SCR), selective catalytic reduction with hydrocarbons (HC-SCR), and the NO_x storage and reduction (NSR) catalyst [2].

An alternative technology under development for NO_x removal is electrochemical $deNO_x$ [3–5], which, compared to the three aforementioned technologies, has the advantage no extra reducing agents needs to be supplied, as the NO is reduced by electrons during polarization. Pancharatnam et al. [6] discovered in 1975 that NO can be reduced to N_2 during polarization in absence of oxygen, and later, it was discovered that NO can also be reduced during polarization in the presence of oxygen [7, 8], which made electrochemical $deNO_x$ of interest for cleaning of oxygen containing exhaust gasses.

Since then, several studies have been carried within electrochemical $deNO_x$ [9–15]; however, the main challenges in the development of electrochemical $deNO_x$ continue to be to achieve a sufficiently high activity and selectivity [5]. In this work, it is attempted to improve the selectivity and activity of the LSF15-CGO10 composite electrodes for electrochemical $deNO_x$ by adding a NO_x storage compound, as known from NSR catalysis, to the electrodes.

The addition of the NO_x storage compound to the electrodes is expected to improve the NO_x, conversion by concentrating the NO_x in the form of nitrates on the electrode surface. Promising results has so far been achieved with combining electrochemical deNO_x and a NO_x storage compound by Nagao et al. [13] and Hamamoto et al. [14]; however, in both cases, the electrode contained platinum. Two important questions arises when adding NO_x storage compound to the electrodes used in this work: (1) As no platinum is present in the electrodes, will the electrode material itself be able to oxidize NO to NO_2, as this step needs to precede the formation of nitrate on the storage compound? (2) How will the presence of a NO_x storage compound alter the electrode processes?

With respect to question (1), Werchmeister et al. [15, 16] has shown electrochemical reduction of NO on LSM ($La_{1-x}Sr_xMnO_3$)–CGO, LSF–CGO, and LSCF ($La_{1-x}Sr_xCo_{1-y}Fe_yO_{3-\delta}$)–CGO electrodes was preceded by catalytically formation of NO_2. For this reason, formation of nitrates for NO_x storage is likely possible, even when platinum is not present on the electrodes used for electrochemical deNO_x.

Question 2 is not easy to answer, but a suggestion can be made for the overall electrode processes, which may be useful to keep in mind during the later interpretation of the results. On a cell without a NO_x storage compound, the expected electrode processes for electrochemical reduction of NO is:

$$\text{Cathode}: \mathrm{NO} + 2\mathrm{e}^- \rightarrow \frac{1}{2}\mathrm{N_2} + \mathrm{O}^{2-} \quad (1)$$

$$\text{Anode}: \mathrm{O}^{2-} \rightarrow \frac{1}{2}\mathrm{O_2} + 2\mathrm{e}^- \quad (2)$$

Note that the equations above state the overall processes and do not take into account any catalytic formation of NO_2. On the cathode a dominating, competing reaction to the reduction of NO is the reduction of O_2: $O_2+4e^-\rightarrow 2O^{2-}$.

When a NO_x storage compound like K_2O/KNO_3 is added to the electrodes, one could imagine the electrode processes to become:

$$\text{Cathode}: 2\,\mathrm{KNO_3} + 10\,\mathrm{e}^- \rightarrow \mathrm{K_2O} + \mathrm{N_2} + 5\,\mathrm{O}^{2-} \quad (3)$$

$$\text{Anode}: 4\mathrm{NO_2} + 2\,\mathrm{K_2O} + 2\,\mathrm{O}^{2-} \rightarrow 4\mathrm{KNO_3} + 4\mathrm{e}^- \quad (4)$$

However, the formation of KNO_3 is not necessarily an electrochemical process as described in the anode equation above, but could just be a chemical reaction: $4NO_2+2K_2O+O_2\rightarrow 4KNO_3$ as in conventional NSR catalysis, in that case O_2 could be supplied from oxidation of the O^{2-} at the anode or from the surrounding atmosphere. An improved performance for electrochemical deNO_x could eventually be gained by repeatedly changing the current direction through the cell and thereby making the electrodes act alternately as cathodes and anodes, as shown by Hibino et al. [17] and Hamamoto et al. [14]. However, such experiments were not made in this work, since the available test setup did not allow for precise measurements of the effect of alternating polarization on the gas composition.

In this work, three different LSF15–CGO10 cell stacks were tested with respect to conversion of NO_x in the temperature range of 300–500 °C. The stacks were subjected to electrochemical impedance spectroscopy and conversion/polarization experiments, while the gas composition was monitored by a mass spectrometer (MS) and a chemiluminescense detector. The cell stacks differed from each other in the way they were impregnated: One stack had no impregnation, one stack was impregnated with KNO_3, and one stack was impregnated with K_2O. LSF was chosen as electrode material, since LSF as a mixed conductor [18][19] has been evaluated to be a promising material for intermediate temperate solid oxide electrodes [20] while CGO was chosen as an electrolyte, as CGO has superior oxygen ion conductivity below 600 °C when compared to yttria-stabilized zirconia [21]. KNO_3/K_2O was chosen for impregnation, as potassium is known to act both as a NO_x storage compound [22] and also to improve simultaneous NO_x and soot removal [23, 24], the latter being of interest for future development of the electrochemical deNO_x technique. With respect to the development of the electrochemical deNO_x technique, it must emphasized that the work presented in this paper is at the very early stage of the development process and only deals with investigated materials ability to electrochemically convert NO_x in model atmospheres containing only NO_x, O_2, and Ar, even though real diesel exhaust also contain significant amounts of CO_2 and H_2O [25]. The presence of CO_2 and H_2O may influence the performance and degradation of the electrochemical deNO_x electrodes. In that context, it is important formation of stable carbonate species does not appear to be a problem on potassium containing catalysts in the presence of NO_x [22, 26], while the influence of H_2O on the potassium-impregnated LSF15–CGO10 electrodes is not clear and will have to be investigated in the future.

Experimental

Fabrication of porous cell stacks

The cell stacks tested in this work were ceramic, porous cell stacks consisting of 11 alternating layers of electrode and electrolyte. The porous stack design was chosen for this work, as the large contact area between

gas and cell in this design makes it easy to measure the NO conversion.

The electrode layers in the porous cell stacks were a LSF15–CGO10 composite with 65 wt% LSF15 and 35 wt % CGO10. The LSF had been synthesized in house by the glycine–nitrate combustion synthesis [27] from nitrate solutions supplied by Alfa Aesar. The LSF15 was synthesized with the exact composition $La_{0.84}Sr_{0.149}FeO_3$. The CGO10 was supplied by Rhodia. For the fabrication of the composite electrode, the LSF15 and CGO10 were mixed with solvent, binder, dispersant, and poreformer (graphite), ball milled and subsequent tapecasted. For more detailed information on the tapecasting procedure, see He et al. [28]. The porous CGO electrolyte was tapecasted like the electrode tape, and afterwards, the green electrode and electrolyte tapes were laminated together with six-electrode layers alternating with five-electrolyte layers. Round cell stacks with a diameter of 18 mm were stamped out of the green laminated tapes and thereafter sintered at 1250 °C. During the sintering the graphite poreformer was burned off leaving behind the pores in the stack. Before testing, a porous Au current collector was applied to the cell stack by painting the outer electrodes with a gold paste containing 20 wt% carbon and subsequent heat the cell stack to 800 °C to decompose the graphite. An image of the 11-layer cell stack with the porous current collector is shown in Fig. 1.

Impregnation

For impregnation of the cell stacks, an aqueous solution of 3.1 M KNO_3 (Alfa Aesar) was prepared. The solution also contained 10 wt% P123 (BASF) with respect to the water. The impregnation was made by covering the cell stack with impregnation solution and then placing the cell stack in a vacuum chamber and evacuate to a pressure below 0.1 mbar for approximately 15 s. Excess impregnation solution was wiped of the surface of the cell stack, and thereafter, the cells were heated to 350 °C to decompose the P123. The cell impregnated with K_2O was prepared in exactly the same way, apart from the cell was heated to 700 °C to decompose the KNO_3 into K_2O.

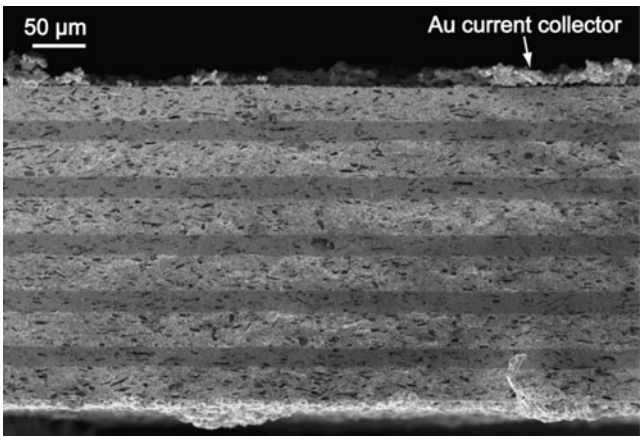

Fig. 1 Cross-section of a non-impregnated LSF15-CGO10 cell stack. The six light gray layers are porous LSF15-CGO10 electrode layers, the five dark gray layers are porous CGO10 electrolyte layers, and on each side of the cell stack, the porous Au current collector is observed (only marked on the top side)

Test setup

For electrochemical cell testing, the stack was mounted in between two alumina tubes, which contained channels for the gas flow and measurement probes for the electrochemical characterization. The cell and the alumina tubes were enclosed in a quartz tube and mounted vertically in a furnace. A sketch of the set-up is shown in Fig. 2.

Electrochemical characterization

A Gamry reference 600 potentiostat was used for the electrochemical characterization of the cell stack. Electrochemical impedance spectra were recorded in the frequency range 1 MHz to 0.001 Hz with 36 mV root mean square amplitude and 6 points per decade. For the conversion experiments the cell stack was first kept at open circuit voltage (OCV) for 2 h, then polarized at −3 V for 2 h and afterwards left at OCV for 2 h again. The electrochemical characterization was made first at 300 °C and then repeated for each 50 °C until 500 °C was reached. After this, the cell was cooled down to 300 °C, one EIS spectrum was recorded to evaluate the degradation during the cell test, and thereafter, the test was finished.

Conversion measurements

The cell stack was supplied with NO, O_2, and Ar from Brooks mass flow controllers. The conversion measurements were

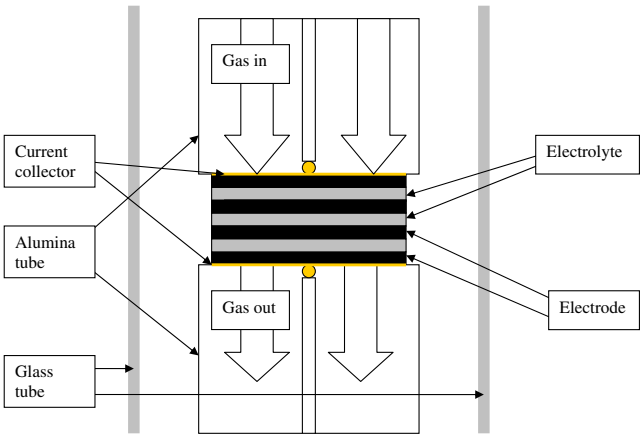

Fig. 2 Sketch of set-up for testing of porous cell stacks (reprinted with permission from [15])

made in 1,000 ppm NO and 1,000 ppm NO+10% O_2 in both cases with balance Ar. These concentrations of NO and O_2 were chosen as they resemble the concentrations that may be found in the exhaust from a diesel car [25]. The NO and NO_2 content in the gas stream from the cell was monitored by a chemilumeniscense detector model 42i high level from Thermo Scientific, while the N_2, N_2O, and O_2 concentration was monitored by a mass spectrometer from Pfeiffer Vacuum, type Omnistar GSD 301.

Scanning electron microscopy

The cell stacks were examined in a Zeiss Supra 35 scanning electron microscope equipped with a field emission gun. SEM images were recorded in two ways: In order to obtain high magnification images of the electrode, microstructure images were recorded with the in-lens detector and 3 keV acceleration voltage on cells just broken and put directly into the microscope. To get more overall images of the cell stacks and the different layers in the stacks, a part of each stack was mounted in epoxy, polished and carbon coated prior to the microscopy investigation.

Results and discussion

Microstructure of electrodes before and after testing

Figure 3 shows the microstructure of the electrodes in the three different tested cell stacks. In the non-impregnated cell stack (Fig. 3a), all the electrode grains appear to have a well-defined shape and very smooth surfaces. In the KNO_3-impregnated cell stack (Fig. 3b), the infiltrated KNO_3 is present around the electrode structure as lumps with a porous looking surface. The porous looking KNO_3 surface is likely due to interaction between the electron beam and the KNO_3, as focusing the electron beam on the KNO_3 altered the look of the KNO_3 lumps. Figure 3b also shows that, even though the KNO_3 is present as big lumps in the electrode, there is still open porosity left for the gas to pass through. The electrode of the cell stack that had been impregnated with KNO_3 and subsequent heated to 700 °C to decompose the KNO_3 into K_2O is shown in Fig. 3c. In the electrode KNO_3 lumps are observed together with other irregular-shaped K_2O grains.

Samples from before and after electrochemical cell testing were mounted in epoxy and examined in the microscope to obtain information about changes in the electrode microstructure during testing. No change due to the testing was observed on the non-impregnated sample. However, both the KNO_3- and the K_2O-impregnated sample showed a significant change in microstructure after the testing. The change in microstructure is best described as the grain size

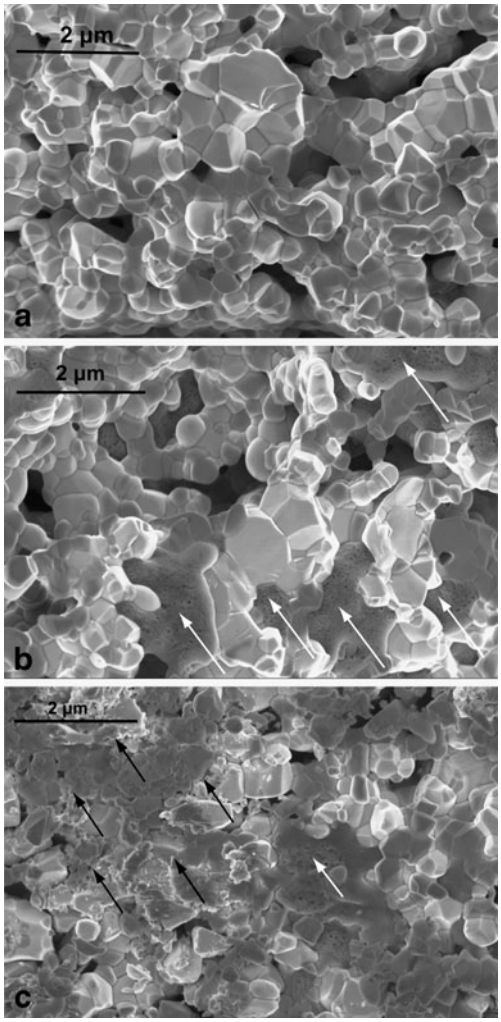

Fig. 3 Microstructure of the electrode of **a** a non-impregnated LSF15-CGO10 cell stack, **b** cell stack impregnated with KNO_3, and **c** cell stack impregnated with KNO_3 and subsequently heated to 700 °C to decompose the KNO_3 into K_2O. *White arrows* point at impregnated KNO_3 and *black arrows* on K_2O

had been reduced and/or the attachments between the electrode grains decreased. The change in microstructure was most pronounced in the outer electrodes of the cell stack and is illustrated in Fig. 4 for the KNO_3 impregnated sample.

Conversion and current efficiency

No purely catalytic effect of the KNO_3 or K_2O impregnation was detected, as no difference between the impregnated and non-impregnated cell stacks was observed in the outlet NO concentration when the stacks before polarization were flushed in either 1,000 ppm NO or 1,000 ppm NO+10% O_2.

In 1,000 ppm NO, zero conversion of NO_x into N_2 during 3 V polarization for 2 h was observed at 300 and 350 °C on the non-impregnated cell stack. However, from 400 to 500 °C the conversion into N_2 increased from 4% to 43% (see Table 1). On the impregnated cell stacks, NO_x conversion in

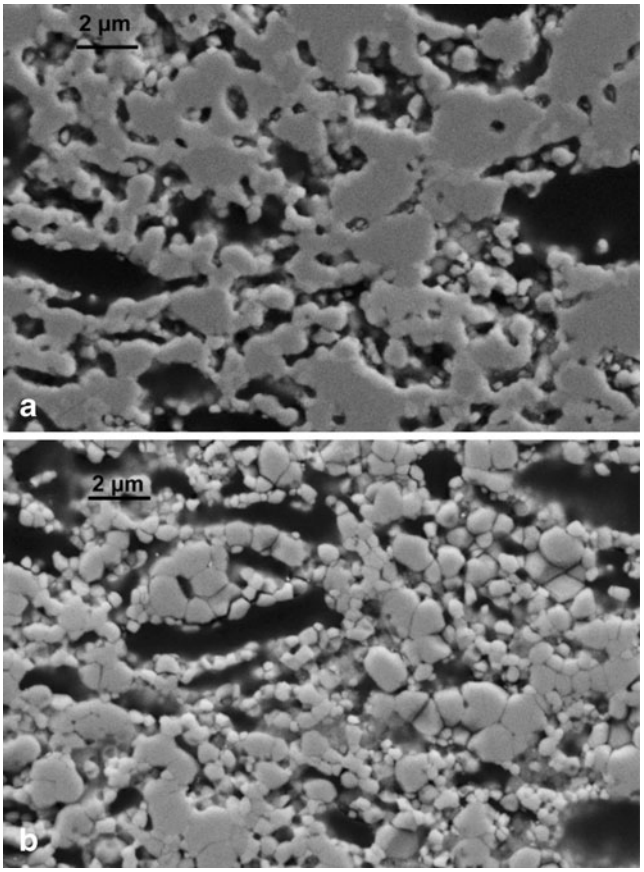

Fig. 4 Outer electrode of KNO_3 impregnated cell stack **a** before electrochemical cell testing and **b** after electrochemical cell testing

the range of 2–17% was observed at 300–350 °C, which means that higher NO_x conversion was observed at low temperatures on the impregnated cell stacks compared to the non-impregnated cell stack. In contradiction to this, the NO_x conversion was lower on the impregnated cell stacks compared to the non-impregnated sample at higher temperatures. A significant decrease in NO_x conversion on the KNO_3-impregnated sample was observed from 350 to 400 °C.

The current efficiency during the 2 h polarization was calculated according to Eq. 5:

$$\text{Current efficiency} = \frac{I_{N_2}}{I_{\text{applied}}} 100\% \quad (5)$$

where I_{N_2} is the current corresponding to the reduction of NO into the N_2, which was detected by the MS, and I_{applied} is the current applied on the cell during the polarization. In Table 2, the current efficiencies in the different tests are stated for the atmosphere with 1,000 ppm NO in Ar. It is observed that impregnation with KNO_3 and K_2O increases the current efficiencies in the temperature range of 300–400 °C. Improved current efficiency at 500 °C is also observed for the K_2O-impregnated sample. The current not used for reduction of NO is used for the competing

Table 1 NO_x conversion (%) for a non-impregnated cell stack, a KNO_3 impregnated cell stack, and a K_2O impregnated cell stack

Temperature (°C)	Non-impregnated	KNO_3 impregnated	K_2O impregnated
300	0	2	3
350	0	17	15
400	4	−1[a]	13
450	15	3	
500	43		15

The cell stack was supplied with 1,000 ppm NO and polarized at −3 V for 2 h. The stated values are the percentage of NO_x converted into N_2.

[a] One percent conversion of NO_x into N_2 corresponds in principle to conversion of N_2 into NO_x. However, since this −1% corresponds to only 4 ppm N_2, it is considered to be within the general uncertainty of the experiment

reduction of O_2. The O_2 likely had been adsorbed on the cell stack during treatment in 10% O_2 in between the polarization experiments or originate from a small leak in the system, as 70–100 ppm $O_{2,\text{leak}}$ was measured by the MS, while the sample was supplied with 1,000 ppm NO in Ar.

In addition to conversion into N_2, oxidation of NO into NO_2 takes place during polarization of the cell stacks in 1,000 ppm NO. In Fig. 5, it is illustrated how the conversion into NO_2 is highest at 300–400 °C for the impregnated cell stacks, whereas for the non-impregnated cell stack, conversion into NO_2 is only observed in the temperature range of 400–500 °C. With respect to the non-impregnated cell stack, a decrease in $O_{2,\text{leak}}$ was observed during polarization/formation of NO_2. The oxygen balance over the blank cell stack at all temperatures showed a deviation below 15 ppm O_2, when comparing the concentrations of NO, NO_2, and $O_{2,\text{leak}}$ before and during polarization. For the impregnated cell stacks, the oxygen balance showed, in general, an excess O_2 concentration during polarization (up to 100 ppm), indicating previously adsorbed O_2 was released from the cell stack during polarization.

When oxygen was present in the atmosphere, conversion of NO_x into N_2 was not observed for any of the samples. It

Table 2 Current efficiency (%) for a non-impregnated cell stack, a KNO_3 impregnated cell stack, and a K_2O impregnated cell stack

Temperature (°C)	Non-impregnated	KNO_3 impregnated	K_2O impregnated
300	0	8	38
350	0	59	73
400	5	−8	37
450	10	4	
500	11		15

The current efficiency is calculated according to Eq. 5. The cell stack was supplied with 1000 ppm NO in Ar and polarized at −3 V for 2 h

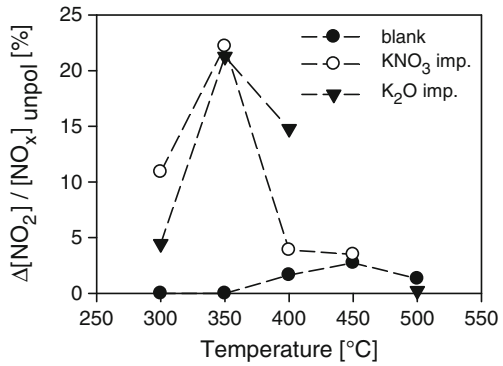

Fig. 5 Conversion of NO into NO_2 relative to the NO_x concentration before polarization in 1000 ppm NO. The cell stacks were polarized at 3 V for 2 h, and the stacks were supplied with 1,000 ppm NO in Ar. The *dashed lines* are for visual guidance only

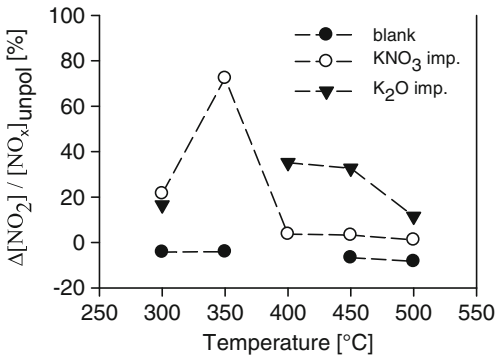

Fig. 7 Relative conversion of NO_2 during 2 h polarization at 3 V on non-impregnated and impregnated LSF cell stacks supplied with 1000 ppm NO + 10% O_2. Positive values correspond to formation of NO_2 and negative values to removal of NO_2. The *dashed lines* are for visual guidance only

should be noted that, even though the gas composition when oxygen was present, in this article, is stated as 1,000 ppm NO+10% O_2, the actual concentration of NO was in the range of 700–900 ppm due to the equilibrium $2\,NO + O_2 \rightleftarrows NO_2$.

Instead of reduction of NO_x into N_2, an increased conversion between NO and NO_2 was observed on the samples during polarization in oxygen containing atmospheres. A significant difference between the cell stack without impregnation and the impregnated stacks was observed: Without impregnation, NO was formed during polarization due to conversion of NO_2, whereas for the samples impregnated with KNO_3 or K_2O, NO_2 was formed during polarization due to conversion of NO. This is clear when Figs. 6 and 7 are compared, where Fig. 6 shows the change in NO concentration during polarization and Fig. 7 shows the change in NO_2 during polarization, in both cases relative to the NO concentration before the samples were polarized. The current through the cell stacks was in 1–20 mA during the polarization at −3 V for both the non-impregnated and the impregnated cell stacks.

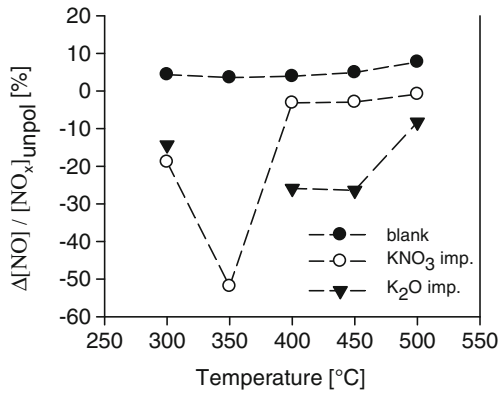

Fig. 6 Relative conversion of NO during 2 h polarization at 3 V on non-impregnated and impregnated LSF cell stacks supplied with 1000 ppm NO + 10% O_2. Positive values correspond to formation of NO and negative values to removal of NO. The *dashed lines* are for visual guidance only

The increased NO conversion due to the presence of potassium observed in this work is in agreement with results reported by Hamamoto et al. [14]. Hamamoto et al. [14] observed increased NO conversion and a decrease in the onset temperature when a potassium-containing adsorbent layer was added to a NiO-YSZ (nickel oxide–yttria-stabilized zirconium oxide) or NiO-CGO-based cell for electrochemical deNO_x. Hamamoto et al. ascribed the increased performance to potassium's ability to adsorb NO and also saw NO decomposition when oxygen was present, which was not observed in this work. The difference could be due to the fact that LSF15–CGO10 electrode used in this work has a larger affinity for O_2 reduction than the NiO-YSZ and NiO-CGO cell used by Hamamoto et al. Another explanation of the increased performance after addition of KNO_3 and K_2O may be the K act as promoter, a phenomenon well-known from heterogeneous catalysis [29]. However, based on the results in this work, it is not possible to distinguish whether the KNO_3 and K_2O mainly improves the performance by increasing the adsorption or by acting as promoters.

With respect to the results obtained in 1,000 ppm NO+ 10% O_2, it should be noted since the current densities are similar for both the non-impregnated and the impregnated cell stacks, but the conversion from NO to NO_2 is higher for the impregnated stacks; the effect of the K species is not to generally increase the performance of the cell stacks, i.e., to increase both the O_2 and the NO conversion, but specifically to increase the NO conversion.

A clear observation in this work was increased NO_2 concentrations during polarization at the temperature range where the largest NO conversion was observed, i.e., in the high temperature range for the non-impregnated samples and in the low temperature range for the impregnated samples. For the non-impregnated electrodes, this likely

show just as reduction of NO into N_2 on the cathodes increases with temperature, so does the oxidation of NO into NO_2 on the anodes of the cell stack. One may speculate if the effect of the KNO_3 and K_2O on the impregnated electrodes only is to act as an NO_x adsorbent or if KNO_3 and K_2O may also facilitate the catalytic formation of NO_2, thereby increasing the total NO_x removal by increasing the concentration of the intermediate NO_2. This is of interest since NO_2 has been identified as an important intermediate for electrochemical reduction of NO_x by Werchmeister et al. [16, 30]. However, according to the literature, K compounds are very poor in catalyzing the oxidation of NO to NO_2 [31]. The most likely explanation of the increased NO_2 level in the low temperature range for the impregnated samples is due to the release of NO_2 during the reduction of the KNO_3 storage compound, as NO_x release is also observed for conventional NSR catalysts during the reduction cycle [32].

The results from the conversion measurements show, at 350 °C, a marked jump in the activity and the current efficiency for the impregnated cells stacks. The temperature 350 °C is above the melting point of KNO_3 (melting point, 334 °C [33]), and the better performance at 350 °C may, for this reason, be due to the presence of molten KNO_3, which may increase the performance by being more mobile compared to solid KNO_3. The performance decrease from 350 °C to higher temperatures may be due to the degradation phenomena, which also caused the degradation of the electrode microstructure as observed on the SEM images.

Effect of impregnation on serial and polarization resistance

The impedance spectra of the non-impregnated cell stack were fitted with the equivalent circuit $R_s(R_1Q_1)(R_2Q_2)(R_3Q_3)$, where R is a resistance, and Q is a constant phase element. For the impregnated cell stacks, the same equivalent circuit was used, apart from some spectra where a fourth (RQ) element had to be included in order to obtain a satisfactory fit. Representative examples of impedance spectra and their deconvolution are shown in Figs. 8, 9, and 10 for the three different samples.

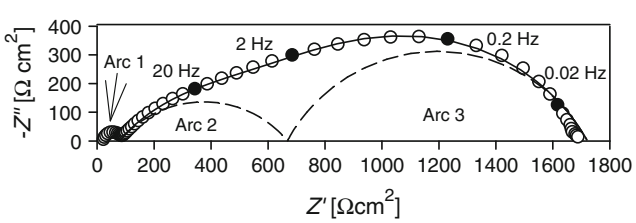

Fig. 8 Impedance spectrum recorded in 1,000 ppm NO+10% O_2 at 400 °C on non-impregnated cell stack. The *solid line* represents the deconvolution of the entire spectrum and the *dashed lines* the deconvolution of the individual processes. For *solid points*, the frequency of the data point is stated

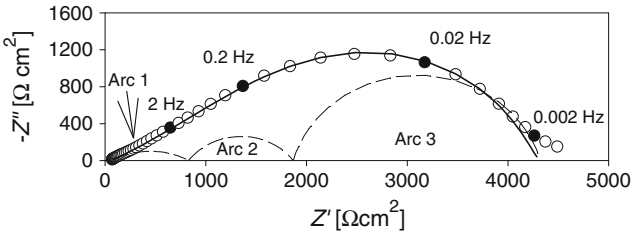

Fig. 9 Impedance spectrum recorded in 1,000 ppm NO+10% O_2 at 400 °C on KNO_3 impregnated cell stack. The *solid line* represents the deconvolution of the entire spectrum and the *dashed lines* the deconvolution of the individual processes. For solid points, the frequency of the data point is stated

The serial resistance (R_s) and polarization resistance (R_p) obtained from the fitting are stated in Table 3. In general, the serial resistances of the impregnated stacks are lower than for the non-impregnated stacks at low temperatures, but higher than for the non-impregnated stacks at higher temperatures.

A possible explanation of the lower serial resistance for the impregnated cell stacks at low temperatures could be improved sintering of the stack due to the presence of potassium [34, 35] or establishment of an easier current pathway through some part of the cell stack. The latter point follows from the conductivities of CGO being ≈0.001 S/cm at 350 °C [21], while the conductivity of the molten KNO_3 at 350 °C is 0.699 S/cm [36], which means that, at 350 °C, the reduced serial resistance observed for the KNO_3-impregnated sample may be explained by the current passing through the KNO_3 instead of the CGO electrolyte. Unfortunately, it has, despite of extensive search, not been possible to find information on the conductivity of K_2O and solid KNO_3 at 300 °C; for this reason, it cannot be estimated here if an alternative current path is a realistic explanation of the reduced serial resistance observed on the impregnated cell stacks at 300 °C. It is also noticed that while the serial resistance of the non-impregnated cell stacks is almost unchanged from the beginning to the end of the cell test, the serial resistance of the impregnated samples increases by a factor of 8–10.

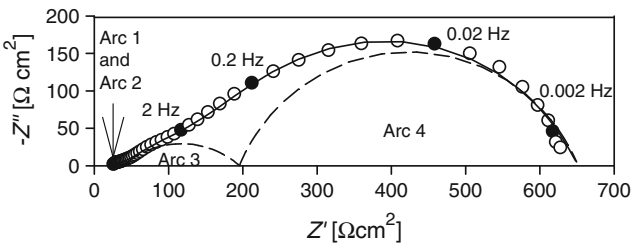

Fig. 10 Impedance spectrum recorded in 1,000 ppm NO+10% O_2 at 400 °C on K_2O impregnated cell stack. The *solid line* represents the deconvolution of the entire spectrum and the *dashed lines* the deconvolution of the individual processes. For solid points, the frequency of the data point is stated

Table 3 Serial resistance (R_s) and polarization resistance (R_p) for three LSF15-CGO10 porous cell stacks without impregnation (non-impregnated), with KNO_3 impregnation and with K_2O impregnation

R_s (Ω cm^2)				R_p (Ωcm^2)		
Temperature (°C)	Non-impregnated	KNO_3 impregnated	K_2O impregnated	Non-impregnated	KNO_3 impregnated	K_2O impregnated
300	140	110	100	5,700		
350	47	110	31	3,200		1,700
400	19	64	20	1,700	4,300	630
450	11	110	16	920	780	190
500	8	40	15	420	210	250
300(post)[a]	140	810	1,000	9,700	24,000	23,000

The cell stacks were supplied with 1,000 ppm NO+10% O_2, while the EIS spectra were recorded

[b] 300(post) refers to the impedance spectra recorded at the end of the experiment, i.e., after temperature variations and polarization experiments had been performed

With respect to the polarization resistance, missing values in Table 3 for the impregnated samples are due to poor quality of the impedance spectra recorded at low temperatures. With one exception, the polarization resistance during the cell test is always lower on the impregnated cell stacks compared to the non-impregnated cell stack. The polarization resistance of the K_2O impregnated sample is between 40% and 80% smaller than the polarization resistance of the non-impregnated cell, even though from 450 to 500 °C, the polarization resistance of the K_2O-impregnated sample starts to increase. With respect to the polarization resistance at 300 °C after the test, the resistance of both the impregnated cell stacks is more than twice the polarization resistance of the non-impregnated cell stack.

The impedance results are consistent with the results from the conversion measurements and the SEM images, as they show that the impregnations not only increase the electrochemical performance of the cell stacks but also cause severe degradation. The degradation causes the pronounced increased in R_s and R_p from the beginning to the end of the test and is related to the breakdown of the electrode microstructure observed on the SEM images. Due to the degradation problems, it was not possible to identify the processes contributing to the polarization resistance of the impregnated cell stacks. However, for the non-impregnated cell stack some of the processes could be identified, as described in the following.

Electrochemical processes in the non-impregnated cell stack

As previously mentioned, the impedance spectra recorded in 1,000 ppm NO+10% O_2 could be fitted with the equivalent circuit $R_s(R_1Q_1)(R_2Q_2)(R_3Q_3)$. The process located at the highest frequency and fitted by the subcircuit (R_1Q_1) had the activation energy of 1 eV and a near-equivalent capacitance of 2×10^{-8} F/cm^2, the near-equivalent capacitance remains constant with temperature. This process was recognized in spectra recorded in all the tree different atmospheres: 1,000 ppm NO+10% O_2, 1,000 ppm NO, and in 10% O_2. The independency on the atmosphere combined with the size of the activation energy identifies the arc as belonging to intrinsic processes in the cell stack, like oxygen ion transport in the electrolyte and across the electrolyte electrode interface [37].

The process located in the middle frequency region in 1,000 ppm NO+10% O_2 has the activation energy of 0.57 eV. The near-equivalent capacitance associated with the process increases with temperature, from 1.7×10^{-5} F/cm^2 at 300 °C to 5.2×10^{-5} F/cm^2 at 500 °C. In 10% O_2, the characteristics of the middle frequency arc were similar, but not totally identical to in 1,000 ppm NO+10% O_2. In 10% O_2, the arc had the activation energy of 0.67 eV, and the capacitance increased with temperature, but a little less steeply compared to in 1,000 ppm NO+10% O_2. The fact that the middle frequency arc depends on the atmosphere indicates the arc may be related to processes like adsorption, diffusion, and charge transfer at or near the triple-phase boundary (TPB) [37]. This also correlates well with the temperature dependency observed for the capacitance, as increasing temperature will increase the TPB zone and thereby increase the associated capacitance. It should be noted that the activation energy in 1,000 ppm NO+10% O_2 is in good agreement with the activation energies reported by Werchmeister et al. [16] for the TPB process in 1% NO on LSF/CGO electrodes. In contradiction to this, the activation energy of 0.67 eV found in 10% O_2 is considerably below the activation energy observed by Werchemister et al. [16] in air, where the activation energies was in the range of 1.2–1.5 eV.

The process located at the lowest frequency has the activation energy 0.52 eV in 1000 ppm NO+10% O_2 and 0.20 eV in 10% O_2. The large discrepancy between the two activation energies indicate that this arc represent two

different processes, depending on whether NO is present in the atmosphere or not. The lack of temperature dependency for the process in 10% O_2 combined with the appearance at the lowest frequencies in the spectrum indicates that this process could be related to gas phase diffusion [37]. The low frequency process when NO is present is likely not a gas phase diffusion process due to the relatively high activation energy observed. In the work by Werchmeister et al. [16], the arc observed at the lowest frequencies in NO containing atmospheres was ascribed to conversion of intermediately formed NO_2. However, for this NO_2 conversion arc, a low activation energy in the range of 0.2–0.3 eV was reported, which makes it unlikely that the arc observed in this work is an NO_2 conversion arc. The best explanation of the low frequency arc is so far it is related to one of the processes dissociative adsorption, surface diffusion, and charge transfer at or near the TPB. One or more of these processes were also expected to account for the middle frequency process observed in this work. It is interesting to note that the activation energies of 0.57 and 0.52 eV found in this work for the middle and low frequency process, respectively, are in good agreement with the activation energies observed by Werchmeister et al. for the TPB related processes on LSF and LSCF electrodes.

Conclusion

In the present work, the effect of KNO_3 and K_2O impregnation on the NO_x conversion on LSF15–CGO10 electrodes was investigated. In an atmosphere only containing 1,000 ppm NO in Ar, impregnation with KNO_3 and K_2O increased the conversion of NO significantly in the temperature range of 300–350 °C. Increased NO_2 concentration was observed in the temperature range where the cell stacks were most active, i.e., for the impregnated cell stacks, the highest NO_2 concentration were observed in the low temperature range, and for the non-impregnated cell stack, the highest NO_2 concentrations were observed in the high temperature range.

When oxygen was present in the atmosphere together with the NO, neither the non-impregnated nor the impregnated cell stacks were able to convert NO_x into N_2. However, a marked difference was observed between the non-impregnated and the impregnated cell stacks in 1,000 ppm NO+10% O_2, whereas the non-impregnated cell stack converted NO into NO_2 under polarization, the impregnated cell stacks converted NO_2 into NO under polarization.

The impregnation with KNO_3 and K_2O overall decreased the polarization resistance of the cell stacks but also introduced severe degradation problems into the stack, as breakdown of the electrode microstructure was observed. Due to the degradation, it was not possible to identify the processes contributing to the polarization resistance of the impregnated stacks. However, for the non-impregnated stack, oxygen-ion transport and TPB-related processes were found to dominate the polarization resistance in 1000 ppm NO+10% O_2.

Further experiments are needed to clarify how KNO_3 and K_2O impregnation affects the NO_x conversion under polarization, among this the role of NO_2 in the reaction mechanism. In addition, the exact cause of the increased degradation observed on impregnated samples is currently not well understood.

Acknowledgments This work was supported by the Danish Strategic Research Council under contract no. 09-065183. Colleagues at the Fuel Cell and Solid State Chemistry Division, Technical University of Denmark, are thanked for help and fruitful discussions.

References

1. Wark K, Warner CF, Davis WT (1998) Air pollution its origin and control, 3rd edn. Addison Wesley Longman, Boston
2. Skalska K, Miller JS, Ledakowicz S (2010) Sci Total Environ 408:3976–3989
3. Stoukides M (2000) Catal Rev - Sci Eng 42:1–70
4. Bredikhin S, Hamamoto K, Fujishiro Y, Awano M (2009) Ionics 15:285–299
5. Hansen KK (2005) Appl Catal, B 58:33–39
6. Pancharatnam S, Huggins RA, Mason DM (1975) J Electrochem Soc 122:869–875
7. Cicero DC, Jarr LA (1990) Sep Sci Technol 25:1455–1472
8. Hibino T (1994) Chem let 5:927–930
9. Walsh KJ, Fedkiw PS (1997) Solid State Ionics 104:97–108
10. Hibino T, Ushiki K, Kuwahara Y, Mizuno M, Mazegi A, Iwahara H (1995) J Chem Soc Faraday Trans 91:1955–1959
11. Hansen KK, Christensen H, Skou EM (2000) Ionics 6:340
12. Bredikhin S, Matsuda K, Maeda K, Awano M (2002) Solid State Ionics 149:327–333
13. Nagao M, Yoshii T, Hibino T, Sano M, Tomita A (2006) Electrochem Solid-State Lett 9:J1–J4
14. Hamamoto K, Fujishiro Y, Awano M (2008) J Electrochem Soc 155:E109–E111
15. Werchmeister RML, Hansen KK, Mogensen M (2010) Mater Res Bull 45:1554–1561
16. Werchmeister RML, Hansen KK, Mogensen M (2010) J Electrochem Soc 157:P107–P112
17. Hibino T, Inoue T, Sano M (2000) Solid State Ionics 130:19–29
18. Teraoka Y, Zhang HM, Okamoto K, Yamazoe N (1988) Mater Res Bull 23:51–58
19. Patrakeev MV, Bahteeva JA, Mitberg EB, Leonidov IA, Kozhevnikov VL, Poeppelmeier KR (2003) J Solids State Chem 172:219–231
20. Ralph JM, Rossignol C, Kumar R (2003) J Electrochem Soc 150: A1518–A1522
21. Dalslet B, Blennow P, Hendriksen PV, Bonanos N, Lybye D, Mogensen M (2006) J of Solid State Electrochem 10:547–561
22. Lesage T, Saussey J, Malo S, Hervieu M, Hedouin C, Blanchard G, Daturi M (2007) Appl Catal, B 72:166–177
23. Teraoka Y, Kanada K, Kagawa S (2001) Appl Catal, B 34:73–78
24. Shangguan WF, Teraoka Y, Kagawa S (1998) Appl Catal, B 16:149–154
25. Kaspar J, Fornasiero P, Hickey N (2003) Catal Today 77:419–449

26. Zhang Z, Zhang Y, Su Q, Wang Z, Li Q, Gao X (2010) Environ Sci Technol 44:8254–8258
27. Chick LA, Pederson LR, Maupin GD, Bates JL, Thomas LE, Exarhos GJ (1990) Mater Lett 10:6–12
28. He Z, Bohm K, Keel AL, Nygaard FB, Menon M, Hansen KK (2009) Ionics 15:427–431
29. Chorkendorff I, Niemantsverdriet JM (2003) Concepts of modern catalysis and kinetics. Wiley-VCH, Weinheim
30. Werchmeister RML, Hansen KK, Mogensen M (2010) J Electrochem Soc 157:P35–P42
31. Toops TJ, Smith DB, Partridge WP (2006) Catal Today 114:112–124
32. Epling WS, Yezerets A, Currier NW (2007) Appl Catal, B 74:117–129
33. Haynes WM,Lide DR (2010-2011) CRC handbook of chemistry and physics, 91st edn. Taylor and Francis, Boca Raton
34. Bruno J, Cavalheiro A, Zaghete M, Varela J (2006) Ceram Int 32:189–194
35. Nzihou A, Adhikari B, Pfeffer R (2005) Ind Eng Chem Res 44:1787–1794
36. Janz GJ (1967) Molten salts handbook. Academic, New York
37. Jørgensen MJ, Mogensen M (2001) J Electrochem Soc 148:A433–A442